

A correspondence between the models of Hodgkin-Huxley and FitzHugh-Nagumo revisited

Eugene B. Postnikov^{1,a} and Olga V. Titkova²

¹ Department of Theoretical Physics, Kursk State University, Radishcheva st. 33, Kursk 305000, Russia

² Department of Mathematical Analysis and Applied Mathematics, Kursk State University, Radishcheva st. 33, Kursk 305000, Russia

Received: 22 August 2016 / Revised: 2 November 2016

Published online: 24 November 2016 – © Società Italiana di Fisica / Springer-Verlag 2016

Abstract. We present the discussion on the possibility to scale the classical dimensionless FitzHugh-Nagumo model of neuronal self-sustained oscillations to the range of variables corresponding to the results, which are provided by the biophysically relevant reduced two-dimensional Hodgkin-Huxley equations (the Rinzel model). It is shown that there exists a relatively simple choice of affine transformation, which results in time-dependent solutions, which reproduce with a high accuracy the time course of the recovery variable and the sharp onsets (intervals of fast motions on a phase trajectories) of the voltage spikes. As for the latter, the reasons for unavoidable difference are discussed as well as a necessity of taking into account applied current values during such a scaling procedure.

1 Introduction

The FitzHugh-Nagumo (FHN) model [1,2] is one of the widespread standard models in theoretical neuroscience [3]. Its popularity is based on the possibility to catch basic qualitative features of neuronal oscillations using the relatively simple polynomial ordinary differential equations (ODEs) replacing thus much more complex ODEs of the Hodgkin-Huxley (HH) model [4]. At the same time, there is still no concordance in the question about a sequential transition between these two models, which regularly arose over decades.

Among various existing approaches, one can mention the discussion of a qualitative correspondence between the probability of potassium channels opening and the inverse relaxation time for the FHN recovery variable [5], a cubic approximation for the sodium membrane current based on the fixed values of the gating functions taken at infinite and zero potentials [6], the introduction of “equivalent potentials” instead of the gating variables with an arbitrary (not necessary FHN-like) polynomial right-hand sides of ODEs [7].

A very important step has been done by Rinzel [8], who strictly and accurately reduced the HH model to the simplified two-variable model, which keeps the voltage time course quite accurately. But although this reduction was named FHN-HH model, it still does have a simple polynomial character of the true FHN.

The most general possible approach has been formulated in the review [9] as “During an action potential, the voltage variable of a real neuron varies between roughly -80mV and 20mV , while its duration is about 1 or 2 ms. These numbers allow one to estimate the factors by which the variables x and t^1 have to be rescaled in order to compare simulation results of the FN model² to a spike train of a specific neuron. Other parameters [...] have to be determined by fitting procedures that use the shape of the action potential [...]”. However, the authors themselves did not realize this procedure, leaving two separate considerations — “biological” and “applied mathematical”.

More recently, fitting of the FHN parameters to real-life records has been presented in a number of works, *e.g.* [10–12]. However, they were primarily aimed at an adjustment of model parameters, not at the underlying reasons for replacing HH by FHN (except for a very short discussion in [10]).

Thus, the main goal of this work is to evaluate the procedure of scaling envisaged by Lindner *et al.* and discuss its results within the following line of reasoning: what the values of factors are, which should be multiplied by the

^a e-mail: postnicov@gmail.com

¹ The variables in the FHN model.

² FHN.

standard FHN parameters to reproduce experimentally relevant values for biological neuron; what the intervals of this reproducibility are; which shape features remain and which are lost as a result of the reduction to the FHN model; and what the geometrical reasons for these losses are.

2 Results

2.1 Models

As was mentioned in the introduction, the four-dimensional HH model can be effectively and well motivationally reduced to the Rinzel two-dimensional model, which can be written as follows [8]:

$$\frac{dv}{dt} = I - g_{Na}(1-w)(v - v_{Na})m_{\infty}(v)^3 - g_K(w/S)^4(v - v_K) - g_l(v - v_l) \quad (1)$$

$$\frac{dw}{dt} = \varepsilon(w_{\infty}(v) - w)/\tau(v), \quad (2)$$

where $S = (1 - h_0)/n_0$ and

$$\begin{aligned} w_{\infty}(v) &= g \frac{S}{1 + S^2} [n_{\infty}(v) + S(1 - h_{\infty}(v))], \\ m_{\infty}(v) &= \frac{a_m(v)}{a_m(v) + b_m(v)}, \\ n_{\infty}(v) &= \frac{a_n(v)}{a_n(v) + b_n(v)}, \\ h_{\infty}(v) &= \frac{a_h(v)}{a_h(v) + b_h(v)}, \\ a_m(v) &= 0.1(v + 40) / (1 - \exp(-(v + 40)/10)), \\ b_m(v) &= 4 \exp[-(v + 65)/18], \\ a_h(v) &= 0.07 \exp[-(v + 65)/20], \\ b_h(v) &= 1 / (1 + \exp[-(v + 35)/10]), \\ a_n(v) &= 0.01(v + 55) / (1 - \exp[-(v + 55)/10]), \\ b_n(v) &= 0.125 \exp[-(v + 65)/80], \\ \tau(v) &= 5 \exp[-(v + 100)^2/55^2] + 1. \end{aligned}$$

All numerical values are given in mV and the numerical values of the constants, adjusted to the reproducibility of HH solutions, are $v_{Na} = 50$, $v_K = -77$, $v_l = -54.4$, $g_{Na} = 120$, $g_K = 36$, $g_l = 0.3$, $I = 20$, $h_0 = 0.596$, $n_0 = 0.317$. The corresponding plots of the voltage v and the recovery variable $w = S[n + S(1 - h)]/(1 + S^2)$, which is a weighted sum of HH gating variables, are presented in fig. 1(left).

The FitzHugh-Nagumo model reads as

$$\frac{dx}{dt} = x - \frac{x^3}{3} - y + z, \quad (3)$$

$$\frac{dy}{dt} = \varepsilon(a + x - by). \quad (4)$$

Its solution (corresponding to the conventionally accepted [3] interval of parameters ($a = 0.7$, $b = 0.8$, $\varepsilon = 0.08$), which provides both excitable and oscillatory regimes and $z = 0.8$ corresponding to developed oscillations far from an extra stiff relaxation regime) is shown in fig. 1(right). One can see a sufficient difference in the scales in both magnitudes and periods with respect to the Rinzel model.

2.2 Affine transformation of FHN variables

Here we superpose both solutions (fig. 1) corresponding to the parameters given above by a scaling procedure. The discussion of an inverse problem (parameters determination for the FHN) will be considered further down.

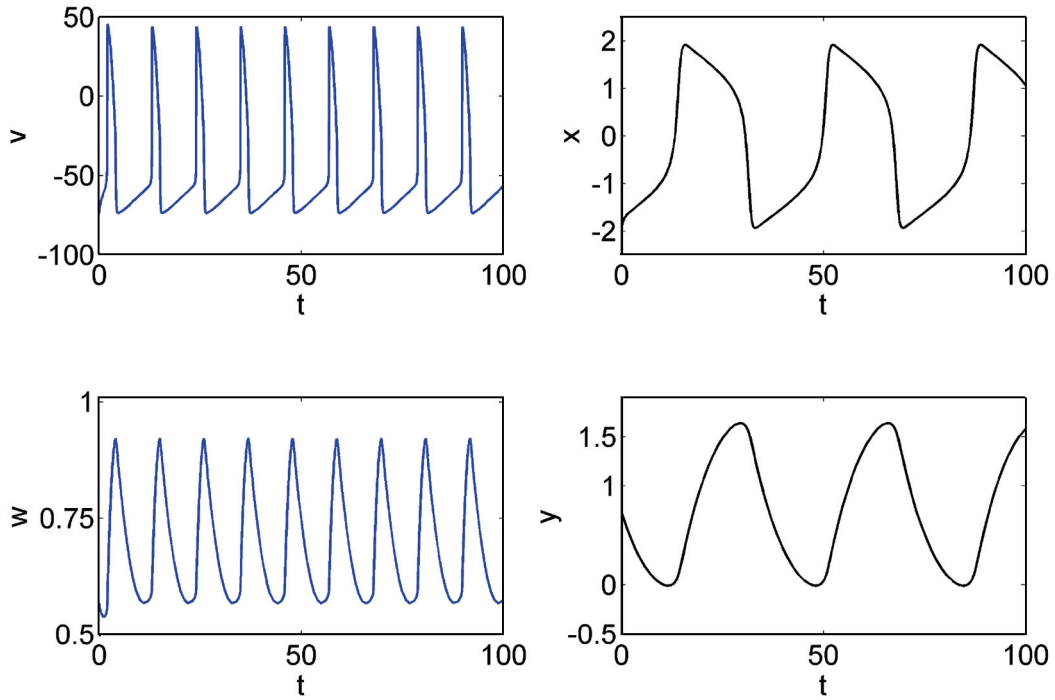


Fig. 1. The original (*i.e.* without any scaling) solutions of the Rinzel (left) and the FHN (right) models.

First of all, we introduce the voltage scaling factor,

$$v_0 = \frac{V_{\max} - V_{\min}}{x_{\max} - x_{\min}}, \tag{5}$$

using maximal and minimal values of the calculated the magnitudes for both the systems. However, we need to note that $|V_{\max}| \neq |V_{\min}|$, *i.e.* these oscillations are quite unsymmetrical with respect to the zero voltage. The asymmetry of the realistic neuronal oscillations described by the Rinzel model originates from the onset potentials of sodium and potassium, whose absolute values are sufficiently different. At the same time, the cubic parabola of the original FHN system is symmetric with respect to the zero potential. Therefore, we need to introduce an appropriate shift $x_0 = (v_{Na} + v_K)/2$. This shift of the parabola's location results also in a modification of the solution for the recovery variable: the replacement $x \rightarrow (x - x_0)/v_0$ needs to be compensated by $a \rightarrow a + x_0/v_0$.

Secondly, Rinzel's recovery variable is sufficiently positive in contrast to the corresponding variable of the FHN. Thus, it is required to repeat the scaling and shift procedure for the recovering variable too. The scaling factor is determined as

$$y_0 = \frac{w_{\max} - w_{\min}}{y_{\max} - y_{\min}}, \tag{6}$$

where y means a solution with this shifted parabola used in the FHN equations and the shift superposing both recovery variables is $y \rightarrow y - y_m$, where $y_m = \min(w) - \min(y)$.

Finally, we consider the time scaling. The corresponding coefficient $\epsilon = T_{\text{FHN}}/T_R$ is simply introduced as the ratio of oscillation periods for Rinzel's T_R and the FHN models (T_{FHN}), since both solutions are periodic. The right-hand sides of eqs. (3) and (4) will be multiplied by this factor due to the rescaling $t \rightarrow \epsilon t$.

Whence, the final scaled and shifted system of the equation takes the form

$$\frac{dx}{dt} = \epsilon \left[(x - x_0) \left(1 - \frac{(x - x_0)^2}{3v_0^2} \right) - (y - y_m) \frac{v_0}{y_0} + zv_0 \right], \tag{7}$$

$$\frac{dy}{dt} = \epsilon \epsilon \left(ay_0 + (x - x_0) \frac{y_0}{v_0} - b(y - y_m) \right), \tag{8}$$

which is obtained from the system (3)-(4) by the affine transformation of its variables

$$\begin{pmatrix} \frac{x - x_0}{v_0} \\ \frac{y - x_m}{y_0} \end{pmatrix} \rightarrow \begin{pmatrix} x \\ y \end{pmatrix}, \quad t \rightarrow \epsilon t. \tag{9}$$

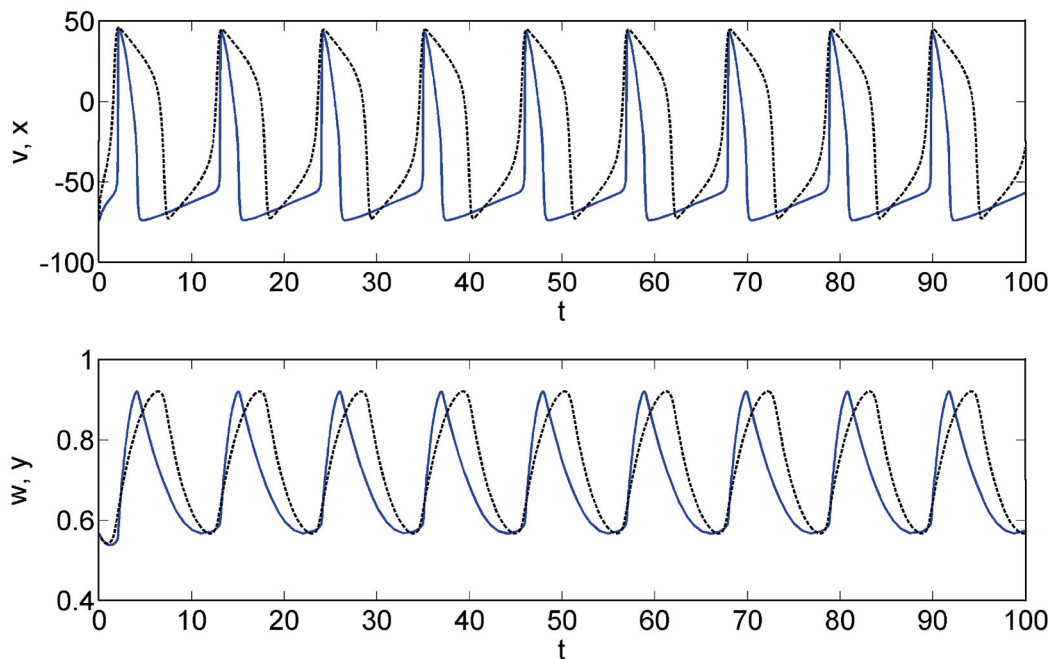


Fig. 2. The solutions of the Rinzel model (blue lines) and the scaled and shifted FHN model (black dashed lines) with the standard parameters and the scaling/shift factors $x_0 = -13.5$, $v_0 = 30.5$, $y_0 = 0.214$, $y_m = 0.569$, $\epsilon = 3.33$.

The solution, which utilizes the affine transformation (9), is shown in fig. 2. One can see that although both curves have now the same scale their shapes still differ a lot. Although the maxima of voltage variable coincide, the width of the FHN solution is much more larger than that of Rinzel's. On the other hand, examination of plots for the recovery variables provides a hint on which parameter needs to be modified to correct the noted discrepancy.

2.3 Adjustment of FHN parameters

The shapes of recovery variables are quite similar (quantitatively, in contrast to the voltages) for both models, but it is obvious that x grows slower than w . Such a behaviour obviously originates from too large self-relaxation of the FHN's recovery variable, *i.e.* a too large value of b . Diminishing its value down to $b = 0.2$ allows for reaching this goal after an appropriate choice of current variable z . The last goal is reached namely by minimizing the squared difference between the solution of (1)-(2) for w and the solutions for y from (7)-(8) computed pointwisely for the arrays representing these numerical solutions.

In details, the fitting procedure, which provides values of the scaling parameters, was evaluated for a set of Rinzel's current values taken from the interval $I \in [20, 100]$ (the step 10 was used) as follows:

- For each I , an appropriate sequence of z_j was taken (with the step 0.01 for $z_j = -0.7 \dots -0.1$, and 0.005 for $z_j = -0.1 \dots 0.1$, respectively).
- For each z_j the scaling procedure was evaluated with respect to the sequence of steps described in subsect. 2.2: the time was scaled by ϵ to fit numerically solution periods of the original form of FHN and Rinzel equations; then the shift of the voltage $x_0 = (v_{Na} + v_K)/2$ was introduced and the scaling factors, v_0 , y_0 , calculated as the ratio of averaged differences between maxima and minima of variables (5), (6), which are numerical solutions of both equations; finally, the displacement of the recovery variable y_m was found equalizing its minimal value for the solution of Rinzel's equation and the solution of the scaled FHN equations with scaling parameters obtained during the previous steps.
- The sums of squared differences between all points of the numerically found solution representing the recovery variable for the Rinzel equation and the scaled FHN equation were found for all z_j , and the value $z_{j_{\min}}$, which corresponds to minimal sum's value, was chosen.
- For this j_{\min} the scaling and shifting parameters were taken; they were represented directly or within a functional form, which visually gives most linear dependence on I , see fig. 3 and its caption, where the mentioned functional forms are written.
- Finally, the procedure of polynomial fit (by the least-square method) was evaluated for these points (linear for all quantities except y_m), where the quadratic polynomial gives better adjustment.

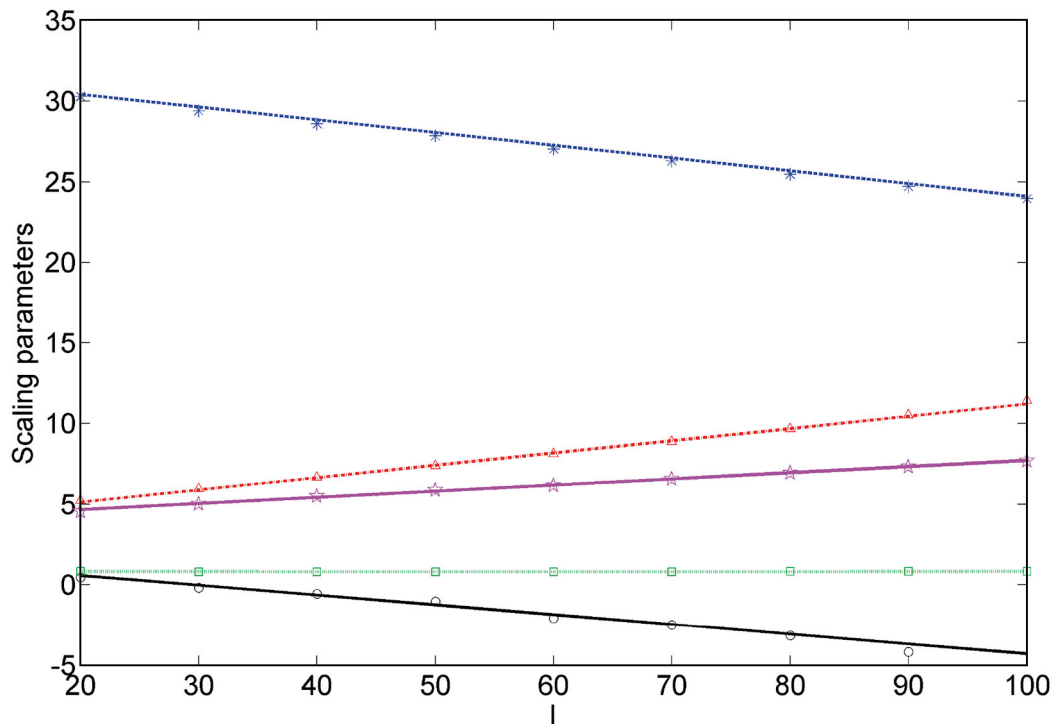


Fig. 3. The fitting procedure: markers represent $\log[(z+1)^{-1} - 1]$ (circles), v_0 (asterisks), y_0^{-1} (triangles), y_m (squares), ϵ (stars), and the straight lines are their least square fitting with the parameters given in eqs. (10)–(14).

Thus, we obtain the following approximations valid within the mentioned interval:

$$z(I) = 1 / [\exp(-0.061I + 1.8) + 1] - 1, \tag{10}$$

$$v_0(I) = -0.079I + 32, \tag{11}$$

$$y_0(I) = (0.076I + 3.6)^{-1}, \tag{12}$$

$$y_m(I) = 1.3 \cdot 10^{-5} I^2 - 0.0015I + 0.85, \tag{13}$$

$$\epsilon(I) = 0.038I + 3.9. \tag{14}$$

They can be used to recalculate results of neurooscillation modelling using the FHN equation (with the cubic parabola shifted on $x_0 = -13.5$ mV, in dimensional form, or on $x_0 = 13.5/v_0$, in dimensionless form, where v_0 is given by eq. (11)) to the dimensional representation, which can be compared with electrophysiological data. Note also that eqs. (10)–(14) are completely self-sufficient expressions, which do not depend on the starting FHN values, and therefore the proposed approximation can be used “as is”, using the applied current as an input parameter only.

Figure 4 shows several examples of these procedures evaluated for different external original currents. One can see that now the curves representing the recovery variables coincide for all considered cases with a high accuracy. Moreover, the onsets of voltage spikes coincide too. As a direct consequence, there is a coincidence of the widths of spikes, which is an important property for usage of the FHN equations for modelling of physiologically realistic neuronal signals. At the same time, the course of pre-spike voltage growth and, to a lesser degree, the details of the first stage of spikes discharges still remain different. The background for this will be discussed in the next section.

3 Discussion

The revealed similarity and difference between details of both solutions can be demonstrably explained via an exploration of phase portraits for two systems (1)-(2) and from (7)-(8), see fig. 5.

One can see that the $dw/dt = 0$ -nullcline is practically linear for $v < -50$; moreover, it is practically parallel to the exactly linear $dy/dt = 0$ -nullcline for small voltage values. At the same time, a curvature of the $dw/dt = 0$ -nullcline within the interval of larger voltages is not so drastic, and the Rinzel system goes through this interval quite quickly, *i.e.* it affects principally v but not w . As a result, this explains why the time solutions for w and the scaled y coincide with a high accuracy, see fig. 4. Thus, the slope of the linear function in (8), v_0/y_0b , can be obtained simply via a

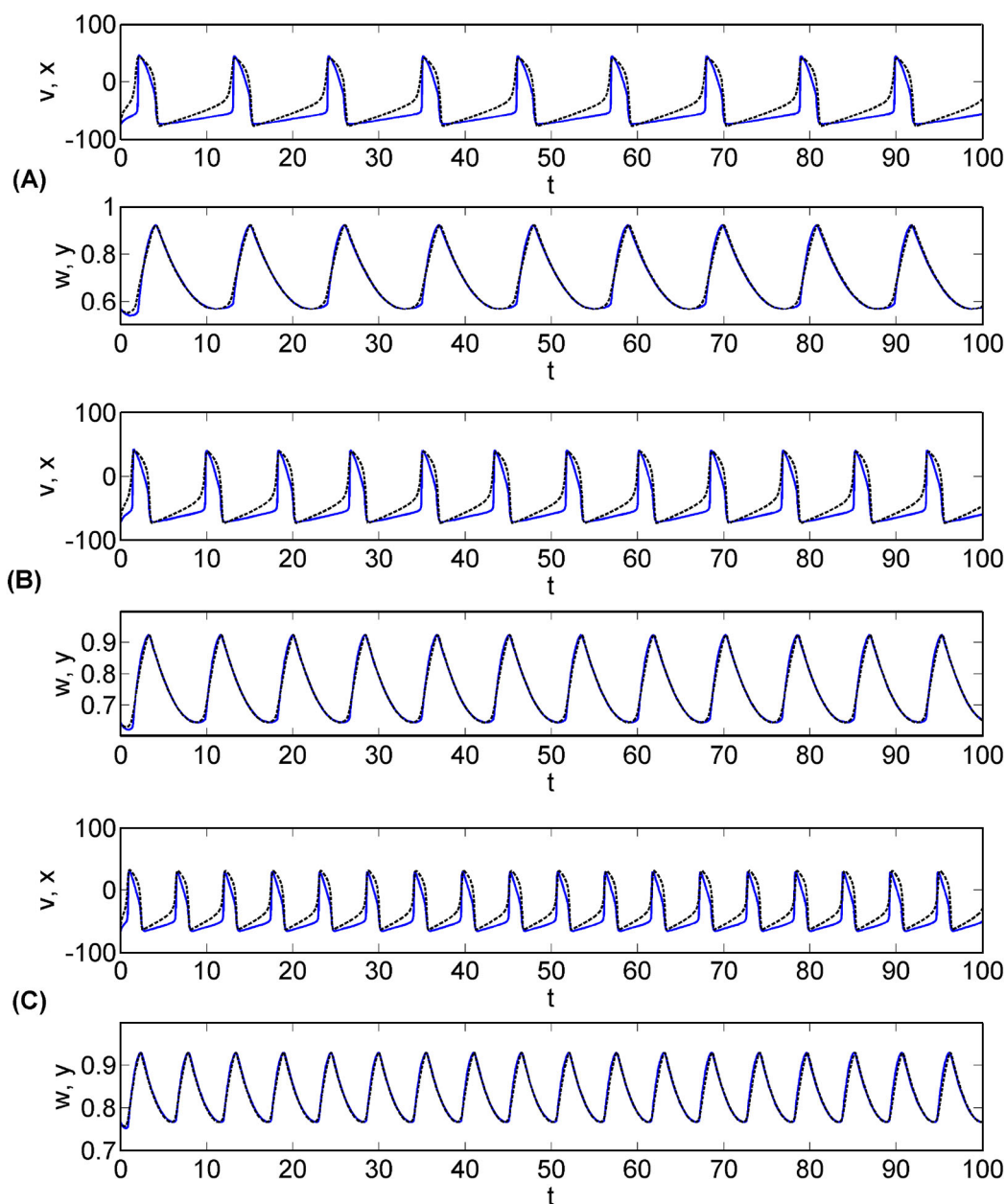


Fig. 4. The solutions of the Rinzel model (blue lines) for $I = 20$ (A), $I = 40$ (B) and $I = 100$ (C), and the scaled and shifted FHN model (black dashed lines) with $b = 0.2$ and $z = -0.61$, $z = -0.36$, and $z = 0$, respectively.

linearisation of the right-hand side of eq. (2). However, the constant shift cannot be determined in such a way, its value is closely connected with the difference between $dv/dt = 0$ - and $dx/dt = 0$ -nullclines.

The characteristic feature of the $dv/dt = 0$ -nullcline is its appreciable asymmetry, with a notable difference of both its “humps” in width. On the contrary, the FHN cubic parabola is exactly antisymmetric. Therefore, it is not possible to obtain a high-quality coincidence between the scaled $x(t)$ and $v(t)$. Especially, this is seen within the slow voltage growth subinterval, where the width difference between the mentioned nullclines is maximal. The nullclines subintervals corresponding to the decaying part of solutions are closer in shape, and the difference between $x(t)$ and $v(t)$ is smaller there, see fig. 4. One can adjust these shapes introducing higher orders of polynomials only [13] but it will not be the FHN model.

Thus, the cubic parabola of the FHN can approximate the Rinzel’s one in “an average sense” only, as has been introduced originally by FitzHugh [1]. Moreover, various local expansions of the exact nullcline in one point [6] cannot provide adequate parameter estimation valid for a wide range of external currents, due to the asymmetry discussed above.

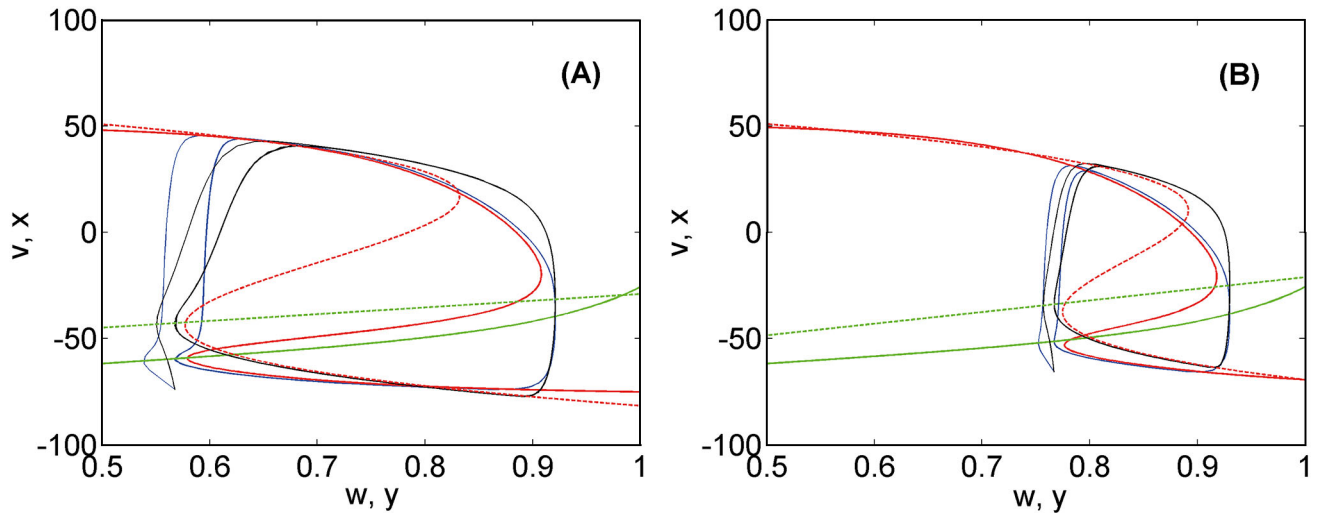


Fig. 5. The phase trajectories of the Rinzel (blue curve) and the scaled FHN (black curve) solutions and the nullclines of these models (red and green, solid and dashed line, respectively) for $I = 20$ (A) and $I = 100$ (B).

On the other hand, the visual exploration of fig. 5 gives a hint on how these “averaged parameters” can be estimated. One can see that Rinzel’s and FitzHugh-Nagumo’s nullclines intersect around voltage values of the sodium and potassium potentials (there is a small difference but one can neglect it as a first approximation). The FHN nullcline,

$$y = \frac{y_0}{v_0} \left[(x - x_0) \left(1 - \frac{(x - x_0)^2}{3v_0^2} \right) - y_m \frac{v_0}{y_0} + zv_0 \right], \tag{15}$$

has, in fact, two unknown parameters: v_0 and the combination $y_m v_0 / y_0 + z v_0$, since the ratio v_0 / y_0 is the already determinable slope of the nullcline corresponding to eq. (8). Whence, one needs two points to find them. These points will be given equalizing y to

$$w = S \sqrt[4]{\frac{I - g_l(v_{Na} - v_l)}{g_K(v_{Na} - v_K)}}, \tag{16}$$

$$w = \frac{I - g_{Na}(v_K - v_{Na}) - g_l(v_K - v_l)}{g_{Na}(v_K - v_{Na})}, \tag{17}$$

obtained as solutions of the algebraic equation corresponding to the right-hand side of (1) for $v = v_{Na}$ and v_K .

It should be pointed out that the values (16) and (17) are current-dependent, and, therefore the same will be true for the parabola’s parameter in (15). This fact explains why the shift/scaling factors (10)–(14) have this dependence, and why attempts to fit at least reasonable widths and maxima/minima of realistic spikes by the FHN with one set of constant coefficients fail in a wide range of external currents.

Finally, the last parameter, which requires to be defined, is an additional shift of the linear nullcline corresponding to eq. (8), which is visible in fig. 5. Now we can conclude that it originates from the shape difference of other nullclines. Since the parameters of the cubic parabola are stated above, the correcting shift can be introduced via the linear analysis of conditions required for instability of the stationary point.

In this sense, it is also interesting to test the behaviour of the scaled/shifted FHN’s solutions in the excitable (non-oscillating) regime in comparison with Rinzel’s one. Figure 6 shows such solutions for $I = 0$ in eqs. (1)–(2) and (7)–(8), where this null current is substituted into (10)–(14).

One can detect several qualitative similarities and dissimilarities with the self-sustained oscillating regimes shown in fig. 4. The main distinction is a visible difference in the values of stationary potentials (almost 20 mV). The stationary values of the recovery differ too but sufficiently slightly, as is expected from the analysis discussed above. The origin of such a behaviour is clear from the phase plane picture, fig. 6(right). Since the stationary point coincides with the intersection of nullclines, the difference between their shapes results in the exhibited shift, and the voltage’s shift is larger because of principal difference between the nullclines of voltage variables as well as the voltage curve shape effects in the oscillatory regime mentioned above.

On the other hand, the regions of phase plane far from the nullclines intersections are affected to lesser degree. As a result, the maximum and the minimum of the excited spike are reproduced by the scaled/shifted FHN quite accurately as well as the spike’s duration and both its onsets. Moreover, the accuracy of this reproduction is even better in comparison with the voltage curves in fig. 4. On the contrary, the “tail” of the relaxing recovery variable exhibits some larger difference but it is connected with the vicinity of the stationary point.

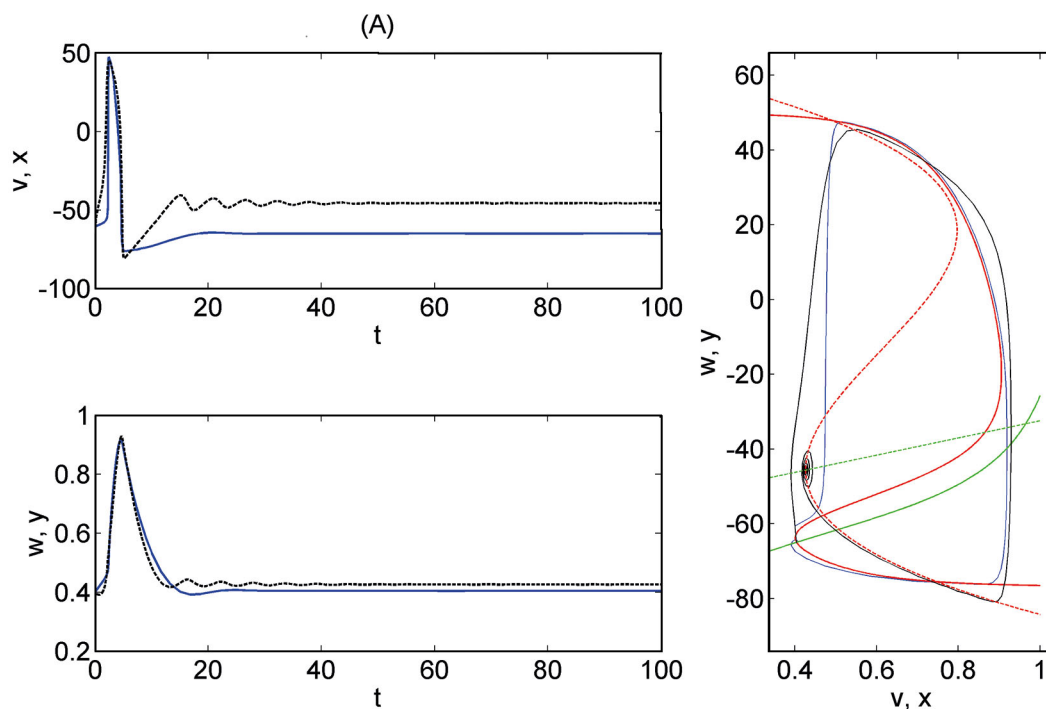


Fig. 6. The solutions of the Rinzel model (blue lines) and the scaled and shifted FHN model (black dashed lines) corresponding to the excitable regime, *i.e.* $I = 0$ and the FHN affine transformation parameters (10)–(14) with this value substituted, as well as their representation on the phase plane (the notation of lines is the same as in fig. 5).

Thus, one can see that the scaled/shifted FHN with the functions of current (10)–(14) allows for operating with neurobiologically relevant shapes and durations of spikes, even in the non-oscillating excitable regime, while one is interested in operating with spikes themselves. The only irreproducible thing is the stationary point value, but it originates from the unavoidable difference between the realistic and the symmetric cubic nullclines.

4 Conclusion

In this work, we evaluated the sequential scaling of the FitzHugh-Nagumo model aimed at reproducing principal features of the time course of neurophysiological oscillations. The last ones were modelled by the Rinzel model, which represents the Hodgkin-Huxley model reduced to two variables. It is shown that the appropriate scaling allows for the reproducing the magnitude and width of the voltage spikes (although there are some discrepancies in the shape before both onsets of spikes) and the time evolution of the recovering variables, which is reproduced with a high accuracy. The explicit current-dependent expressions for the shift and scaling factors are provided. They can be used for recalculation of dimensionless FHN-based models to dimensional ones, which can be compared with experimental data and vice versa, since the considered affine transformations are invertible.

The additional semi-quantitative analysis based on the phase plane representation gave some estimations for the range of these factors and argued that the mutual mapping between these kinds of models should take into account the applied external current.

Note, finally, that the approach of replacing the H-H equations by the FHN equations scaled in such a way that they preserve a shape of spikes may be useful not only from the methodological point of view but also when applied to some modern problems connected with the modelling of neurovascular coupling mediated by glia [14]. Within this problem, the reproducibility not only of oscillations frequency but also of the shape of spikes could be crucial since neuronal oscillations interact with the neuroglial subsystem controlled by calcium dynamics and vasomotor activity, which exhibit excitable and oscillating dynamics too [15,16].

For this reason the comprehensive recent models [17–19] combine the Hodgkin-Huxley model for neurons with more simple kinetic equations for other counterparts. At the same time, it is shown that even the classic FHN equations can serve as building blocks for this problem [20,21]. Thus, the proposed modification of the FHN equations, which keep them simple for numerical simulations but provides time dependences accurately resembling the same quantities of H-H (Rinzel's) model, may be a candidate for large-scale simulations in this field of study.

EBP is partially supported by the Russian Science Foundation, project 16-15-10252.

References

1. R. FitzHugh, *Biophys. J.* **1**, 445 (1961).
2. J. Nagumo, S. Arimoto, S. Yoshizawa, *Proc. IRE* **50**, 2061 (1962).
3. E.M. Izhikevich, R. FitzHugh, *Scholarpedia* **1**, 1349 (2006).
4. A.L. Hodgkin, A.F. Huxley, *J. Physiol.* **117**, 500 (1952).
5. A.C. Scott, *Rev. Mod. Phys.* **47**, 487 (1975).
6. R.G. Casten, H. Cohen, P.A. Lagerstrom, *Q. Appl. Math.* **32**, 365 (1975).
7. T.B. Kepler, L.F. Abbott, E. Marder, *Biol. Cybern.* **66**, 381 (1992).
8. J. Rinzel, *Fed. Proc.* **44**, 2944 (1985).
9. B. Lindner, J. Garca-Ojalvo, A. Neiman, L. Schimansky-Geier, *Phys. Rep.* **392**, 321 (2004).
10. P.E. Phillipson, P. Schuster, *Int. J. Bifurcat. Chaos* **15**, 3851 (2005).
11. Y. Che *et al.*, *Chaos* **22**, 023139 (2012).
12. A. Concha, R. Garrido, *J. Comput. Nonlinear Dyn.* **10**, 021023 (2015).
13. A.C. Ventura, G.B. Mindlin, S.P. Dawson, *Phys. Rev. E* **65**, 046231 (2002).
14. C. Iadecola, *Nat. Rev. Neurosci.* **5**, 347 (2004).
15. M.R. Metea, E.A. Newman, *J. Neurosci.* **26**, 2862 (2006).
16. D.E. Postnov, A.Y. Neganova, J.C.B. Jacobsen, N.-H. Holstein-Rathlou, O. Sosnovtseva, *Eur. Phys. J. ST* **222**, 2667 (2013).
17. R.C. Sotero, R. Martinez-Cancino, *Neural Comp.* **22**, 969 (2010).
18. R. Jolivet, J.S. Coggan, T. Allaman, P.J. Magistretti, *PLoS Comput. Biol.* **11**, e1004036 (2016).
19. K. Chhabria, V.S. Chakravarthy, *Front Neurol.* **7**, 24 (2016).
20. D.E. Postnov, L.S. Ryazanova, O.V. Sosnovtseva, *Biosystems* **89**, 84 (2007).
21. M. Hayati, M. Nouri, S. Haghiri, D. Abbott, *IEEE Trans. Biomed. Circ. Syst.* **10**, 518 (2016).